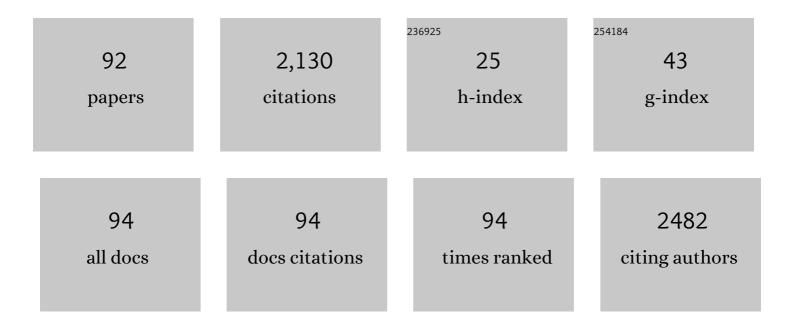
## Zhihong Xu

List of Publications by Year in descending order

Source: https://exaly.com/author-pdf/8997164/publications.pdf Version: 2024-02-01



ZHIHONC XII

#	Article	IF	CITATIONS
1	Surfactant free RGO/Pd nanocomposites as highly active heterogeneous catalysts for the hydrolytic dehydrogenation of ammonia borane for chemical hydrogen storage. Nanoscale, 2012, 4, 5597.	5.6	202
2	A highly sensitive and selective colorimetric and off–on fluorescent chemosensor for Cu2+ based on rhodamine B derivative. Sensors and Actuators B: Chemical, 2011, 156, 546-552.	7.8	168
3	Synthesis, characterization, and DNA-binding properties of the cobalt(II) and nickel(II) complexes with salicylaldehyde 2-phenylquinoline-4-carboylhydrazone. Journal of Photochemistry and Photobiology A: Chemistry, 2008, 196, 77-83.	3.9	107
4	New pyrrole-based single-molecule multianalyte sensor for Cu2+, Zn2+, and Hg2+ and its AIE activity. Sensors and Actuators B: Chemical, 2018, 255, 3085-3092.	7.8	77
5	Study on synthesis, structure, and DNA-binding of Ni, Zn complexes with 2-phenylquinoline-4-carboylhydrazide. Journal of Inorganic Biochemistry, 2009, 103, 210-218.	3.5	75
6	Synthesis of Au nanorod-embedded and graphene oxide-wrapped microporous ZIF-8 with high electrocatalytic activity for the sensing of pesticides. Nanoscale, 2019, 11, 7839-7849.	5.6	62
7	Spectroscopic studies on binding of 1-phenyl-3-(coumarin-6-yl)sulfonylurea to bovine serum albumin. Journal of Photochemistry and Photobiology B: Biology, 2008, 92, 98-102.	3.8	58
8	Analysis of Binding Interaction between Bovine Serum Albumin and the Cobalt(II) Complex with Salicylaldehyde-2-phenylquinoline-4-carboylhydrazone. Chemical and Pharmaceutical Bulletin, 2009, 57, 1237-1242.	1.3	56
9	A novel colorimetric and ratiometric fluorescent Cu2+ sensor based on hydrazone bearing 1,8-naphthalimide and pyrrole moieties. Sensors and Actuators B: Chemical, 2017, 251, 813-820.	7.8	55
10	Fluorescent graphene oxide composites synthesis and its biocompatibility study. Journal of Materials Chemistry, 2012, 22, 9308.	6.7	54
11	An AIRE active Schiff base bearing coumarin and pyrrole unit: Cu2+ detection in either solution or aggregation states. Sensors and Actuators B: Chemical, 2018, 260, 106-115.	7.8	54
12	A novel ratiometric colorimetric and NIR fluorescent probe for detecting Cu2+ with high selectivity and sensitivity based on rhodamine-appended cyanine. Sensors and Actuators B: Chemical, 2014, 201, 469-474.	7.8	50
13	An "off-on―fluorescein-based colormetric and fluorescent probe for the detection of glutathione and cysteine over homocysteine and its application for cell imaging. Sensors and Actuators B: Chemical, 2018, 260, 295-302.	7.8	48
14	AEE active Schiff base-bearing pyrene unit and further Cu2+–induced self-assembly process. Sensors and Actuators B: Chemical, 2018, 258, 393-401.	7.8	47
15	Quinoline-based hydrazone for colorimetric detection of Co2+ and fluorescence turn-on response of Zn2+. Spectrochimica Acta - Part A: Molecular and Biomolecular Spectroscopy, 2020, 230, 118025.	3.9	41
16	Rhodamine-2-thioxoquinazolin-4-one conjugate: A highly sensitive and selective chemosensor for Fe 3+ ions and crystal structures of its Ag(I) and Hg(II) complexes. Sensors and Actuators B: Chemical, 2017, 239, 60-68.	7.8	39
17	A highly sensitive and selective off–on fluorescent chemosensor for hydrazine based on coumarin β-diketone. Spectrochimica Acta - Part A: Molecular and Biomolecular Spectroscopy, 2018, 188, 80-84.	3.9	38
18	A novel â€~turn-on' coumarin-based fluorescence probe with aggregation-induced emission (AIE) for sensitive detection of hydrazine and its imaging in living cells. Spectrochimica Acta - Part A: Molecular and Biomolecular Spectroscopy, 2019, 222, 117272.	3.9	38

**Z**ніномс Xu

#	Article	IF	CITATIONS
19	Synthesis, characterization, DNA interaction and antibacterial activities of two tetranuclear cobalt(II) and nickel(II) complexes with salicylaldehyde 2-phenylquinoline-4-carboylhydrazone. Inorganic Chemistry Communication, 2011, 14, 1569-1573.	3.9	33
20	Ratiometric fluorescent probe based on pyrrole-modified rhodamine 6G hydrazone for the imaging of Cu2+ in lysosomes. Spectrochimica Acta - Part A: Molecular and Biomolecular Spectroscopy, 2019, 212, 121-127.	3.9	33
21	A highly sensitive and selective colorimetric and off–on fluorescent chemosensor for Cu2+ based on rhodamine 6G hydrazide bearing thiosemicarbazide moiety. Journal of Photochemistry and Photobiology A: Chemistry, 2017, 335, 10-16.	3.9	31
22	A pyrazole-containing hydrazone for fluorescent imaging of Al3+ in lysosomes and its resultant Al3+ complex as a sensor for Fâ^'. Talanta, 2019, 203, 178-185.	5.5	31
23	An ESIPT-Based Fluorescent Probe for Hydrazine Detection in Aqueous Solution and its Application in Living Cells. Journal of Fluorescence, 2017, 27, 679-687.	2.5	30
24	Synthesis, characterization, and DNA-binding properties of copper(II), cobalt(II), and nickel(II) complexes with salicylaldehyde 2-phenylquinoline-4-carboylhydrazone. Transition Metal Chemistry, 2008, 33, 267-273.	1.4	27
25	Novel rhodamine-based colorimetric and fluorescent sensor for the dual-channel detection of Cu2+ and Co2+/trivalent metal ions and its AIRE activities. Spectrochimica Acta - Part A: Molecular and Biomolecular Spectroscopy, 2019, 212, 1-9.	3.9	27
26	AIE active salicylaldehyde-based hydrazone: A novel single-molecule multianalyte (Al3+ or Cu2+) sensor in different solvents. Spectrochimica Acta - Part A: Molecular and Biomolecular Spectroscopy, 2019, 212, 146-154.	3.9	26
27	Three salicylaldehyde derivative Schiff base ZnII complexes: synthesis, DNA binding and hydroxyl radical scavenging capacity. Transition Metal Chemistry, 2007, 32, 564-569.	1.4	25
28	A simple hydrazone as a multianalyte (Cu <sup>2+</sup> , Al <sup>3+</sup> , Zn <sup>2+</sup> ) sensor at different pH values and the resultant Al <sup>3+</sup> complex as a sensor for F <sup>â^'</sup> . RSC Advances, 2018, 8, 5640-5646.	3.6	25
29	Palladiumâ€Catalyzed C(sp2)–H Bond Alkylation of Ketoximes by Using the Ringâ€Opening of Epoxides. European Journal of Organic Chemistry, 2016, 2016, 3090-3096.	2.4	24
30	A novel hemicyanine-based near-infrared fluorescent probe for Hg2+ ions detection and its application in living cells imaging. Dyes and Pigments, 2020, 173, 107951.	3.7	24
31	Rapid Detection of <i>Listeria monocytogenes</i> in Raw Milk with Loopâ€Mediated Isothermal Amplification and Chemosensor. Journal of Food Science, 2011, 76, M611-5.	3.1	21
32	Quinoline containing acetyl hydrazone: An easily accessible switch-on optical chemosensor for Zn2+. Spectrochimica Acta - Part A: Molecular and Biomolecular Spectroscopy, 2018, 188, 324-331.	3.9	21
33	Sensitive and selective fluorescent probe for hypochlorite in 100% aqueous solution and its application for lysosome-targetable cell imaging. Spectrochimica Acta - Part A: Molecular and Biomolecular Spectroscopy, 2020, 231, 118110.	3.9	20
34	ICT-modulated NIR water-soluble fluorescent probe with large Stokes shift for selective detection of cysteine in living cells and zebrafish. Spectrochimica Acta - Part A: Molecular and Biomolecular Spectroscopy, 2021, 246, 119030.	3.9	20
35	A turn-on chemosensor for Hg2+ in aqueous media and its application in "MCT―imaging in living cells. Dalton Transactions, 2011, 40, 6382.	3.3	19
36	Aggregation-induced ratiometric emission active monocarbazone: Ratiometric fluorescent probe for Cu2+ in either solution or aggregation states. Journal of Luminescence, 2018, 204, 289-295.	3.1	19

**ZHIHONG XU** 

#	Article	IF	CITATIONS
37	Highly Sensitive and Selective Fluorescent Probe for Detection of Fe3+ Based on Rhodamine Fluorophore. Journal of Fluorescence, 2019, 29, 645-652.	2.5	18
38	Isolation, structure elucidation, tyrosinase inhibitory, and antioxidant evaluation of the constituents from Angelica dahurica roots. Journal of Natural Medicines, 2020, 74, 456-462.	2.3	18
39	Hydrazone derivative bearing coumarin for the relay detection of Cu2+ and H2S in an almost neat aqueous solution and bioimaging in lysosomes. Spectrochimica Acta - Part A: Molecular and Biomolecular Spectroscopy, 2021, 255, 119693.	3.9	18
40	A deep-red lysosome-targetable fluorescent probe for detection of hypochlorous acid in pure water and its imaging application in living cells and zebrafish. Spectrochimica Acta - Part A: Molecular and Biomolecular Spectroscopy, 2022, 264, 120270.	3.9	18
41	A highly sensitive and selective fluorescent probe for Hg2+ and its imaging application in living cells. Inorganic Chemistry Communication, 2013, 34, 42-46.	3.9	17
42	A NIR sensor for cyanide detection and its application in cell imaging. Spectrochimica Acta - Part A: Molecular and Biomolecular Spectroscopy, 2018, 199, 141-145.	3.9	17
43	Pyrrole-quinazoline derivative as an easily accessible turn-off optical chemosensor for Cu2+ and resultant Cu2+ complex as a turn-on sensor for pyrophosphate in almost neat aqueous solution. Spectrochimica Acta - Part A: Molecular and Biomolecular Spectroscopy, 2020, 226, 117592.	3.9	16
44	A simple hydrazone as a fluorescent turn-on multianalyte (Al3+, Mg2+, Zn2+) sensor with different emission color in DMSO and resultant Al3+ complex as a turn-off sensor for Fâ^ in aqueous solution. Journal of Luminescence, 2019, 212, 191-199.	3.1	15
45	CTAB assisted immobilization of RuO <sub>2</sub> nanoparticles on graphene oxide for electrochemical sensing of hydrazine. Fullerenes Nanotubes and Carbon Nanostructures, 2017, 25, 435-441.	2.1	14
46	Molecularly imprinted polymers fabricated by Pickering emulsion polymerization for the selective adsorption and separation of quercetin from Spina Gleditsiae. New Journal of Chemistry, 2019, 43, 14747-14755.	2.8	14
47	A pyrrole-containing hydrazone and its Cu <sup>2+</sup> complex: an easily accessible optical chemosensor system for the successive detection of Zn <sup>2+</sup> /Cu <sup>2+</sup> and pyrophosphate. Analytical Methods, 2018, 10, 5790-5796.	2.7	13
48	Crystal structure, biological studies of water-soluble rare earth metal complexes with an ofloxacin derivative. Inorganica Chimica Acta, 2012, 384, 324-332.	2.4	12
49	An indole–rhodamine-based ratiometric fluorescent probe for Pd <sup>2+</sup> determination and cell imaging. Analytical Methods, 2019, 11, 1080-1086.	2.7	12
50	Highly sensitive and selective ESIPT-based near-infrared fluorescent probe for detection of Pd2+. Inorganic Chemistry Communication, 2019, 101, 135-141.	3.9	12
51	A near-infrared colorimetric and fluorescent dual-channel probe for cyanide detection based on dicyanomethylene-4H-pyran. Inorganic Chemistry Communication, 2020, 122, 108245.	3.9	11
52	Two new phenylethanoid glycosides from Ginkgo biloba leaves and their tyrosinase inhibitory activities. Carbohydrate Research, 2020, 494, 108059.	2.3	11
53	A ratiometric fluorescent probe for hydrogen sulfide in neat aqueous solution and its application in lysosome-targetable cell imaging. Spectrochimica Acta - Part A: Molecular and Biomolecular Spectroscopy, 2022, 270, 120835.	3.9	10
54	Synthesis, crystal structure, and DNA-binding of a 3-D netlike supramolecular manganese picrate complex with 2,6-bis(benzimidazol-2-yl)pyridine. Journal of Coordination Chemistry, 2010, 63, 1097-1106.	2.2	9

**ZHIHONG XU** 

#	Article	IF	CITATIONS
55	Simple thiosemicarbazone "switch" sensing of Hg2+ and biothiols in pure aqueous solutions and application to imaging in lysosomes. Journal of Molecular Structure, 2022, 1250, 131811.	3.6	9
56	A supramolecular self-assembly host–guest system from cyclodextrin as an absolute water-soluble fluorescence sensor for aluminium ions: synthesis, characterization and sensing activity. RSC Advances, 2017, 7, 38160-38165.	3.6	8
57	Insights into Ag( <scp>i</scp> )-catalyzed addition reactions of amino alcohols to electron-deficient olefins: competing mechanisms, role of catalyst, and origin of chemoselectivity. RSC Advances, 2018, 8, 40338-40346.	3.6	8
58	An AIRE-active far-red ratiometric fluorescent chemosensor for specifically sensing Zn2+ and resultant Zn2+ complex for subsequent pyrophosphate detection in almost pure aqueous media. Spectrochimica Acta - Part A: Molecular and Biomolecular Spectroscopy, 2021, 263, 120169.	3.9	8
59	A water soluble hydrazone probe for subsequent fluorescent detection of Zn2+ and S2â^' in neat aqueous solution and imaging in mitochondria of living cells. Journal of Molecular Structure, 2022, 1249, 131629.	3.6	8
60	A water-soluble lysosome-targetable fluorescent probe for carboxylesterase detection and its application in biological imaging. Dyes and Pigments, 2022, 199, 110079.	3.7	8
61	Oneâ€Pot Functionalization of 8â€Aminoquinolines through the Acylation and Regioselective C5â€H Halogenation under Transitionâ€Metalâ€Free Conditions. ChemistrySelect, 2019, 4, 13964-13967.	1.5	7
62	A 1,8-naphthalimide-based turn-on fluorescent probe for imaging Cu2+ in lysosomes. Inorganic Chemistry Communication, 2021, 134, 109026.	3.9	7
63	NHC-Catalyzed Transformation Reactions of Imines: Electrophilic versus Nucleophilic Attack. Journal of Organic Chemistry, 2022, 87, 7989-7994.	3.2	7
64	Development of a semiacenaphthenofluorescein-based optical and fluorescent sensor for imaging cysteine in cells. Journal of Photochemistry and Photobiology A: Chemistry, 2020, 386, 112090.	3.9	6
65	Rhodamine hydrazone as a lysosome-targetable pH biomarker for the selective differentiation of cancer cells from normal cells. Inorganic Chemistry Communication, 2020, 122, 108260.	3.9	6
66	A simple hydrazone probe for recognition of Al3+ and PPi and its applicability in lysosomal imaging. Spectrochimica Acta - Part A: Molecular and Biomolecular Spectroscopy, 2022, 268, 120680.	3.9	6
67	Synthesis and characterization of a novel Anderson-type tungstotellurate decorated by transition metal complexes: [Na(H2O)3]2[{Cu(2,2′-bipy)2}2(TeW6O24)]·Â4H2O. Transition Metal Chemistry, 2008, 3237-241.	331,.4	5
68	Electrochemical Oxidation Cross Dehydrogenative Coupling of Enamines and Thiophenols for the Synthesis of Vinyl Sulfides. ChemistrySelect, 2021, 6, 6460-6463.	1.5	5
69	A quinoline-based probe for the ratiometric fluorescent detection of sulfite in lysosomes of living cells. Spectrochimica Acta - Part A: Molecular and Biomolecular Spectroscopy, 2022, 275, 121160.	3.9	5
70	A novel indene-chalcone-based fluorescence probe with lysosome-targeting for detection of endogenous carboxylesterases and bioimaging. Spectrochimica Acta - Part A: Molecular and Biomolecular Spectroscopy, 2022, 278, 121329.	3.9	5
71	2-[(5-Chloro-2-hydroxybenzylidene)amino]-3′,6′-bis(diethylamino)spiro[isoindoline-1,9′-xanthen]-3-one. Acta Crystallographica Section E: Structure Reports Online, 2010, 66, o1500-o1500.	0.2	4
72	2-[(2,4-Dihydroxybenzylidene)amino]-3′,6′-bis(ethylamino)spiro[isoindoline-1,9′-xanthen]-3-one. Acta Crystallographica Section E: Structure Reports Online, 2010, 66, 01504-01504.	0.2	4

**ZHIHONG XU** 

#	Article	IF	CITATIONS
73	A Novel Water Cluster Held Up by a Tungstotellurate of the [Ni(2,2'-bipy)3]2+ Cations: Synthesis and Characterization of [Ni(2,2'-bipy)3]2[H2(TeW6O24)]·28H2O. Synthesis and Reactivity in Inorganic, Metal Organic, and Nano Metal Chemistry, 2012, 42, 140-144.	0.6	4
74	Six Natural Phenylethanoid Glycosides: Total Synthesis, Antioxidant and Tyrosinase Inhibitory Activities. ChemistrySelect, 2020, 5, 10817-10820.	1.5	4
75	Thiocarbazoneâ€appended coumarin: An easily accessible ratiometric fluorescent chemosensor for multianalyte (Zn <sup>2+</sup> and Cu <sup>2+</sup> ) systems. Coloration Technology, 2022, 138, 157-167.	1.5	4
76	A pyrazine-containing hydrazone derivative for sequential detection of Al3+ and Fâ^'. Journal of Molecular Structure, 2022, 1251, 132073.	3.6	4
77	Andersonâ€Evans Type Tungstotellurate with Metalâ€Organic Complex Moieties: Preparation, Structure and Properties of Na2[Co(C12H8N2)3]2[TeW6O24]·A25ÂA·Â16H2O. Synthesis and Reactivity in Inorganic, Mo Organic, and Nano Metal Chemistry, 2006, 36, 687-692.	etal6	3
78	3′,6′-Bis(ethylamino)-2′,7′-dimethyl-2-{[2-[(E)-3,4-methylenedioxybenzylideneamino]ethyl}spiro[isoino Acta Crystallographica Section E: Structure Reports Online, 2009, 65, o1876-o1876.	doline-1,9	′-xanthen
79	Synthesis and Structure of a Novel Two-dimensional Manganese(II) Azide Complex with N-Methylimidazole. Analytical Sciences: X-ray Structure Analysis Online, 2007, 23, X175-X176.	0.1	2
80	Synthesis and Crystal Structure of 2-Furanyl-2-phenylquinoline-4-carboxylhydrazone. Analytical Sciences: X-ray Structure Analysis Online, 2007, 23, X203-X204.	0.1	2
81	Preparation, characterization, and catalytic performance of a novel methyl-rich Ti-HMS mesoporous molecular sieve with high hydrophobicity. Science China Chemistry, 2010, 53, 1337-1345.	8.2	2
82	Regioselective Dechloroacetylations Mediated by Ammonium Acetate: Practical Syntheses of 2,3,4,6â€Tetra―O â€chloroacetylâ€glycopyranoses and Cinnamoyl Glucose Esters. ChemistrySelect, 2020, 5, 6360-6364.	1.5	2
83	Crystal Structure of a New POM-based Organic-Inorganic Hybrid: {[Cu(2,2'-bipy)Cl]2}n{[Na5(H2O)14](TeMo6O24)}n 2nH2O. Analytical Sciences: X-ray Structure Analysis Online, 2007, 23, X235-X236.	0.1	1
84	Synthesis and Crystal Structure of Two Novel Tungstotellurates with Metal-Organic Complex Moieties. Synthesis and Reactivity in Inorganic, Metal Organic, and Nano Metal Chemistry, 2008, 38, 657-663.	0.6	1
85	Crystal Structure of a Novel Binuclear Copper(II) Complex with 2-(Methoxycarbonyl)benzoic Acid. Analytical Sciences: X-ray Structure Analysis Online, 2008, 24, X303-X304.	0.1	1
86	Synthesis and Crystal Structure of 1-Cyclopropyl-6-fluoro-7-hydrozino-8-methoxyl-1,4-dihydro-4-oxo-3-quinoline carbohydrazide. X-ray Structure Analysis Online, 2009, 25, 19-20.	0.2	1
87	3-[(Furan-2-ylmethylidene)amino]-1-(4-methylphenyl)thiourea. Acta Crystallographica Section E: Structure Reports Online, 2011, 67, o275-o275.	0.2	0
88	1-Benzylideneamino-3-(4-methylphenyl)thiourea. Acta Crystallographica Section E: Structure Reports Online, 2011, 67, o449-o449.	0.2	0
89	3′,6′-Bis(ethylamino)-2′,7′-dimethyl-2-{2-(E)-[(thiophen-2-yl)methylideneamino]ethyl}spiro[isoindoline methanol monosolvate. Acta Crystallographica Section E: Structure Reports Online, 2012, 68, o1556-o1556.	e-1,9′-x; 0.2	anthen]-3-on 0
90	7-[(5,5-Dimethyl-2-oxido-1,3,2-dioxaphosphinan-2-yl)oxy]-4-methyl-2H-chromen-2-one. Acta Crystallographica Section E: Structure Reports Online, 2012, 68, o1924-o1924.	0.2	0

#	Article	IF	CITATIONS
91	Crystal structure of dinitrato-(N′-((quinolin-8-yl)methylene)isonicotinohydrazide κ3-N,N′,O)copper(II), C16H12N6O7Cu. Zeitschrift Fur Kristallographie - New Crystal Structures, 2018, 233, 309-310.	0.3	ο
92	Crystal structure of Diiodo-(N′-((quinolin-8-yl)methylene)isonicotinohydrazide κ3N,N′,O)cadium(II) – dimethylformamide (1/1), C19H19N5O2CdI2. Zeitschrift Fur Kristallographie - New Crystal Structures, 2018, 233, 307-308.	0.3	0